Published OnlineFirst June 16, 2009; DOI: 10.1158/1541-7786.MCR-08-0402

Calcineurin A–Binding Protein, a Novel Modulator of the Calcineurin-Nuclear Factor of Activated T-Cell Signaling Pathway, Is Overexpressed in Wilms' Tumors and Promotes Cell Migration

Alana H.T. Nguyen, Mélanie Béland, Yaned Gaitan, and Maxime Bouchard

Goodman Cancer Centre and Department of Biochemistry, McGill University, Montreal, Quebec, Canada

Abstract

Current therapeutic strategies against Wilms' tumor (WT) reach 80% to 85% success rate. In spite of this, a remaining 15% to 20% of tumors relapse and are associated with increased metastasis and poor prognosis. To identify new regulators of WT progression, we screened for developmental target genes of Pax2, a key regulator of kidney development and a WT signature gene. We show that one of these target genes, *calcineurin A–binding protein* (*CnABP*), is coexpressed with *Pax2* during kidney development and is overexpressed in >70% of WT samples analyzed. The *CnABP* gene encodes a novel protein product conserved in higher vertebrates. We show that CnABP promotes cell proliferation and migration in cell culture experiments. Biochemical analyses additionally identified an interaction between CnABP and calcineurin Aβ, the catalytic subunit of the calcium-responsive serine/threonine phosphatase calcineurin. We show that this interaction leads to the inhibition of calcineurin phosphatase activity and prevents nuclear factor of activated T-cell (NFAT) nuclear translocation. Inhibition of NFAT nuclear localization results in decreased NFAT transcriptional response. Together, these data identify a new modulator of calcineurin signaling up-regulated in WTs. (Mol Cancer Res 2009;7(6):821–31)

Introduction

Wilms' tumors (WT) represent ~85% of childhood kidney cancer. It is believed to arise from nephrogenic rests resulting from a failure of mesenchymal progenitor cells to differentiate into nephrons. This concept is supported by both histologic and molecular data as the tumors typically contain all three cell types derived from mesenchymal progenitor cells (blastemal, epithelial, and stromal; ref. 1) and present a molecular signature consistent with an early kidney differentiation program (2). In this respect, WTs are a classic example of cancer resulting from developmental anomalies.

WTs can be treated with relatively high efficiency. However, 15% to 20% of WT patients experience relapse associated with resistance to treatments and poor prognosis (3, 4). An increased probability of relapse and mortality correlates with anaplasia and metastasis (5, 6) as well as increased chromosomal anomalies (7, 8). At the molecular level, relapse has been linked to consistent deregulation of a limited number of genes, including components of the calcineurin signaling pathway (9).

Evidence for both loss-of-function and gain-of-function mutations has been associated with WT development. *Wilms' Tumor gene 1* (*WT1*) was the first gene identified with genomic alterations or point mutations (10-13) and accounts for 10% to 15% of WTs (14, 15). Consistently with the developmental origin of WTs, *WT1* is expressed in the mesenchymal progenitor cells (metanephric mesenchyme) and is required for its normal differentiation into nephrons (16-18).

The transcription factor PAX2 is ectopically expressed in most WT samples. Initially described for a few tumors (19, 20), the consistent expression of PAX2 and its close family member PAX8 was subsequently observed in several other primary tumor samples (2, 21). A large-scale gene expression analysis further identified *PAX2* as one of the signature genes for WTs (2).

Among the data supporting a functional link between PAX2 and WT development is the close connection between the murine *Pax* genes and *Wt1*, both at the transcriptional level and in terms of cellular functions such as mesenchymal-epithelial transition and cell survival. During the development of the definitive kidney (metanephros), *Pax2* is up-regulated concomitantly with *Wt1* expression in the mesenchymal progenitor cells before the epithelialization of the forming nephron (22). In addition, both genes seem to regulate each other at the transcriptional level (22, 23). As Wt1, Pax2 plays a crucial role in the initiation of metanephric kidney induction and nephron formation in the embryo (24). Later during development, Pax2 is involved in nephron maturation (25) and is shut down in terminally differentiated nephrons.

Expression of *PAX* genes in cancer correlates with reduced apoptosis as well as increased proliferative and invasive phenotypes (26-29). Inhibition of *PAX2* in renal cell lines reduces proliferation as well as resistance to cisplatin treatment (26, 28). Analyses of the $Pax2^{+/-}$ kidney phenotype also support a role

Received 8/28/08; revised 3/5/09; accepted 3/7/09; published OnlineFirst 6/16/09.
Grant support: National Cancer Institute of Canada grant 015121. A.H.T. Nguyen is the recipient of a studentship from the Canadian Institutes for Health Research. M. Béland is a recipient of KRESCENT/Canadian Institutes for Health Research Post-Doctoral Fellowship. M. Bouchard holds a Canada Research Chair in Developmental Genetics of the Urogenital System.
The costs of publication of this article were defrayed in part by the payment of page charges. This article must therefore be hereby marked *advertisement* in accordance with 18 U.S.C. Section 1734 solely to indicate this fact.
Note: Supplementary data for this article are available at Molecular Cancer Research Online (http://mcr.aacrjournals.org/).
Requests for reprints: Maxime Bouchard, Goodman Cancer Centre and Department of Biochemistry, McGill University, 1160 Pine Avenue West, Montreal, Quebec, Canada H3A 1A3. Phone: 514-398-3532; Fax: 514-398-6769. E-mail: maxime.bouchard@mcgill.ca

doi:10.1158/1541-7786.MCR-08-0402

Published OnlineFirst June 16, 2009; DOI: 10.1158/1541-7786.MCR-08-0402

for Pax2 in cell survival (30-33). Expression of PAX2 correlates with increased migration of Kaposi sarcoma cells and endothelial cells isolated from renal tumors (29, 34). Despite the association of PAX2 and other PAX transcription factors to cancer, little is known about the downstream pathways they regulate.

The consistent misexpression of PAX2 in WTs suggests a role in tumor initiation and/or progression (35). In a screen designed to isolate Pax2 target genes involved in normal and abnormal kidney development, we identified a gene coexpressed with *Pax2* in the mesenchymal progenitor cells at the onset of metanephric kidney development. This gene encodes a membrane-anchored protein, which we named calcineurin A–binding protein (CnABP). Like *PAX2, CnABP* is overexpressed in most WT samples analyzed. Complementary gain-of-function and loss-of-function experiments in cell culture support a role for CnABP in promoting cell proliferation and migration. We finally show that CnABP binds and inhibits calcineurin Aβ, a central component of the calcium signaling pathway identified as a signature pathway of recurrent WTs.

Results

Identification of CnABP

In an effort to find new regulators of kidney development and tumorigenesis, we did a series of microarray experiments comparing (*a*) wild-type with *Pax2* mutant renal cells, (*b*) early with later stages of mouse mesonephros (embryonic kidney) development, and (*c*) *Pax2*-expressing renal cells with surrounding *Pax2*-negative tissues (36, 37). Because *Pax* genes were found as signature markers for WTs and were previously shown to regulate the tumor suppressor gene *Wt1*, we examined our microarray results for genes potentially involved in WT. This was done by mapping differentially regulated expressed sequence tags (EST) to their chromosomal position in the mouse and comparing their syntenic position in human with known putative WT loci (e.g., 11p15, 1p35, 17q, and 16q; ref. 38). As expected, we identified *Wt1*, thereby validating the microarray approach used. Interestingly, we also identified an EST (AK076656) that showed 2.1-fold down-regulation in the absence of *Pax2*, 3.1-fold higher expression in the kidney than in surrounding tissues, and a 3.6-fold up-regulation in time between early and late mesonephros development (Table 1). Using the human and mouse UniGene databases, we found that EST AK076656 corresponds to a novel gene, which we name *CnABP* (see below), located on chromosome 16q in human.

CnABP Is Regulated by PAX2 In vitro and Is Coexpressed with PAX2 in the Developing Kidney

To validate our microarray data, we mapped various potential PAX2-binding sites (PBS) in the *CnABP* locus based on promoter proximity and sequence conservation. Three putative sites were cloned upstream of a luciferase reporter construct and tested for induction by PAX2 (Fig. 1A). Of the three sites tested, only PBS2 exhibited a significant ($P < 0.001$) induction by PAX2 (Fig. 1B). We next introduced point mutations in this site to show the activity of PAX2 on this putative binding site. As expected, PBS2 mutation significantly ($P < 0.01$) reduced the activity of this enhancer element, although residual activity remained. Next, we wanted to validate whether the expression pattern of *CnABP* was compatible with *Pax2* expression at different stages of mouse kidney development. *In situ* hybridization analysis at 12 days of embryonic development (E12.5) detected *CnABP* expression in the ureter as well as in the nephrogenic mesenchyme surrounding the ureter tip (Fig. 1D). This expression pattern was maintained until the end of embryonic development (E18.5) and was extended to differentiating nephrons (Fig. 1E). Importantly, the expression pattern of *CnABP* in the developing kidney overlaps with that of *Pax2* (Fig. 1F and G). Hence, *CnABP* is regulated by Pax2 and expressed in the developing kidney, notably in the nephrogenic mesenchyme, believed to give rise to WTs.

Sequence and Structure of the Human CnABP Gene

According to the human UniGene database, CnABP is expressed as two major isoforms. Isoform-a is composed of three exons and represent ~80% of *CnABP* EST sequences in human. Isoform-b extends and terminates exon 2 within intron 2 of isoform-a (Fig. 2A). This isoform, which corresponds to the mouse Riken clone 4732415M23Rik, was present in <20% of human UniGene ESTs. PCR on reverse-transcribed cDNA of WT and normal kidney samples revealed the expression of isoform-a, whereas isoform-b could not be detected (Fig. 2B). As it is the most prominent isoform, only isoform-a was studied further (Fig. 2B). *CnABP* isoform-a transcript is 2.2 kb long and encodes for a predicted 15.5-kDa protein. To identify paralog sequences for CnABP in mouse or human, we did blast analysis in National Center for Biotechnology Information databases. This search failed to reveal any paralog to *CnABP* in these species. In contrast, Blast analysis against vertebrate amino acid sequences revealed highly conserved domains between CnABP orthologs in mammals (Fig. 2C). The predicted CnABP protein could not be found in fishes or lower vertebrates. Although none of the conserved domains has been

Table 1. Identification of *CnABP* as a Pax2-Regulated Gene by Microarray Analysis of Mesonephric Cells

	Genotype comparison [wt vs Pax2−/− GFP (+) cells]		Up-regulation in time [GFP (+) cells]		Pro/mesonephros expression [GFP (+) vs GFP (−) cells]
	16s	20s	13s vs 16s	13s vs 20s	20s
CnABP	1.5	2.1	1.5	3.6	3.1
B2M	0.9	1.0	1.0	1.2	1.0

NOTE: Ratios are expressed as control/mutant, later/early, or GFP+/GFP−. The embryonic stages are defined in somite number at E9.5.
Abbreviation: s, somite number.

Published OnlineFirst June 16, 2009; DOI: 10.1158/1541-7786.MCR-08-0402

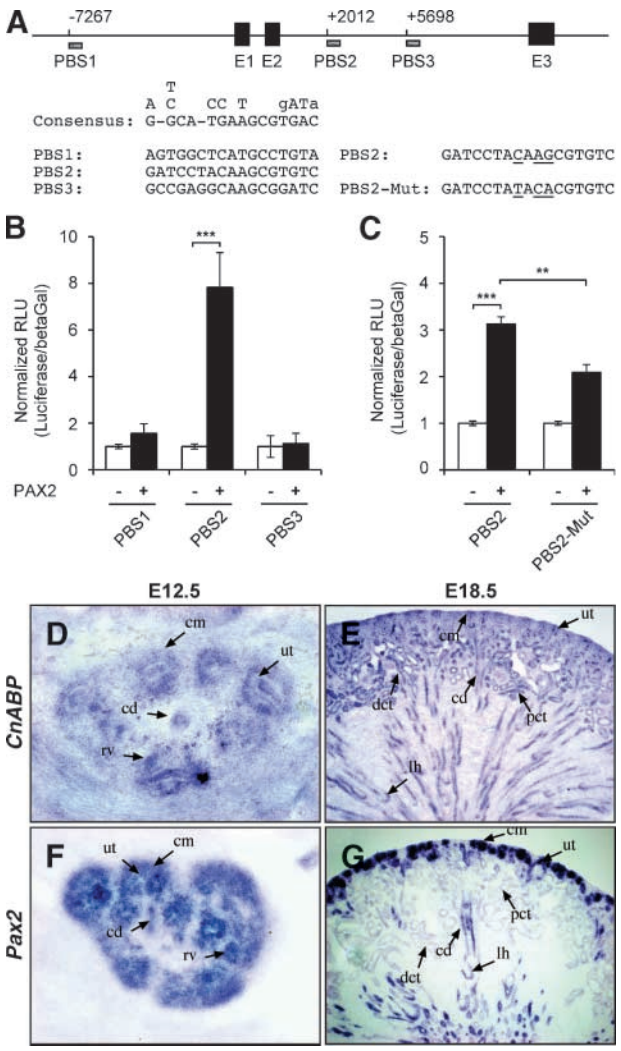

FIGURE 1. Identification of PBSs in the *CnABP* locus and coexpression of *PAX2* and *CnABP* in the mouse kidney. **A.** Three PBSs, PBS1, PBS2, and PBS3 (−7267, +2012, +5698, respectively), were mapped to the *CnABP* locus. These binding sites were tested for reporter gene activation by PAX2. **B.** PAX2 expression did not activate PBS1 and PBS3 but resulted in significant ($P < 0.001$) activation of PBS2. Three critical base pairs within the PBS2 site were mutated to disrupt PAX2 binding (**A**). **C.** Mutating this site resulted in significant reduction ($P < 0.01$) in activation by PAX2 but residual activation remained. *In situ* hybridization with cRNA probes against *CnABP* (**D** and **E**) and *Pax2* (**F** and **G**) was done on mouse embryonic kidneys at E12.5 (**D** and **F**) and E18.5 (**E** and **G**). Both genes are coexpressed in the condensing mesenchyme at the periphery of the kidney surrounding the ureter tips at E12.5. *CnABP* and *Pax2* are maintained in the differentiating nephrons [renal vesicle (*rv*), proximal convoluted tubule (*pct*), loop of Henle (*lh*), and distal convoluted tubule (*dct*)]. cd, collecting duct; cm, condensing mesenchyme; ut, ureter tip. **, $P < 0.01$; ***, $P < 0.001$.

previously annotated, an NH_2-terminal myristoylation consensus site was found. Transfection experiments with green fluorescent protein (GFP)–tagged *CnABP* confirmed that CnABP association with the cell membrane depends on the integrity of this consensus sequence (Supplementary Fig. S1C and D). In addition, a consensus calcineurin docking site (PxIxIT) was identified in the most conserved region of CnABP (Fig. 2C).

CnABP and PAX2 Are Overexpressed in WTs

The overlapping expression of *CnABP* and *Pax2* in the developing kidney led us to hypothesize that, like Pax2, CnABP misexpression may be associated with WT. To test this, we assessed *CnABP* and *PAX2* expression levels in 39 primary WTs relative to normal kidney tissue using quantitative reverse transcription-PCR. In line with previous reports, *PAX2* was found overexpressed in 74% (29 of 39) of these samples (Fig. 3A). Strikingly, *CnABP* expression increased >2-fold the normal levels in 74% of WT samples analyzed (Fig. 3A). As much as 62% of the *CnABP* overexpressing tumors in fact showed >5-fold the normal expression levels. Of the tumors that overexpressed *PAX2*, 83% (24 of 29) also overexpressed *CnABP*. These results establish an association between elevated *CnABP* and *Pax2* expression in WTs. We next assessed expression levels of PAX2 and *CnABP* in tumors with specific loss of heterozygosity (LOH). No association was observed in PAX2 expression level with respect to LOH status (Fig. 3B). However, a high proportion (100%, $n = 10$) of tumors with LOH at 11p exhibit elevated levels of *CnABP* compared with other tumors (Fig. 3C). Hence, *CnABP* is highly expressed in association with *PAX2* in a majority of WTs.

CnABP Promotes Cell Proliferation

To assess whether CnABP has an effect on cell proliferation, we overexpressed *CnABP* in the human embryonic kidney cell line HEK293 and in the WT cell line SKNEP-1 (Supplementary Fig. S2A). HEK293 cells transfected with a *CnABP* expression vector showed higher proliferation rates than cells transfected with vector control (Fig. 4B). After 96 hours in culture, *CnABP*-transfected HEK293 cells had a 50% increase in cell number compared with vector-transfected cells ($P < 0.01$; Fig. 4B). An equivalent 50% increase was also observed in *CnABP*-transfected SKNEP-1 cells compared with control cells at 96 hours ($P < 0.01$; Fig. 4C). To validate the effect of CnABP on cell growth, we knocked down *CnABP* in the renal cell carcinoma cell line ACHN, which expresses both *PAX2* and *CnABP* endogenously (data not shown). Quantitative PCR showed that short hairpin RNA (shRNA) 7202 and 8392 reduced CnABP expression levels by 35% and 75%, respectively (Supplementary Fig. S2C). As expected, CnABP knockdown in ACHN cells resulted in significant reduction in cell growth. shRNA 7202 caused 70% reduction ($P < 0.001$) in cell number after 96 hours, whereas shRNA 8392 resulted in a virtually complete arrest of cell growth ($P < 0.001$; Fig. 4C). Together, these complementary approaches point to an important role of CnABP in regulating cell proliferation.

CnABP Regulates Cell Migration in a Dose-Dependent Manner

To test whether CnABP additionally play a role in cell migration, we transiently transfected HEK293 cells with *CnABP* or vector control and sorted cells according to expression levels of a cotransfected *pEGFP* reporter construct. Western blot analysis confirmed the correlation between CnABP and EGFP expression levels (Supplementary Fig. S2B). Migration assays in Boyden chambers revealed an increase in cell migration that followed CnABP expression levels (Fig. 5A). Cells expressing low CnABP indeed showed a 3-fold increase in cell migration

Published OnlineFirst June 16, 2009; DOI: 10.1158/1541-7786.MCR-08-0402

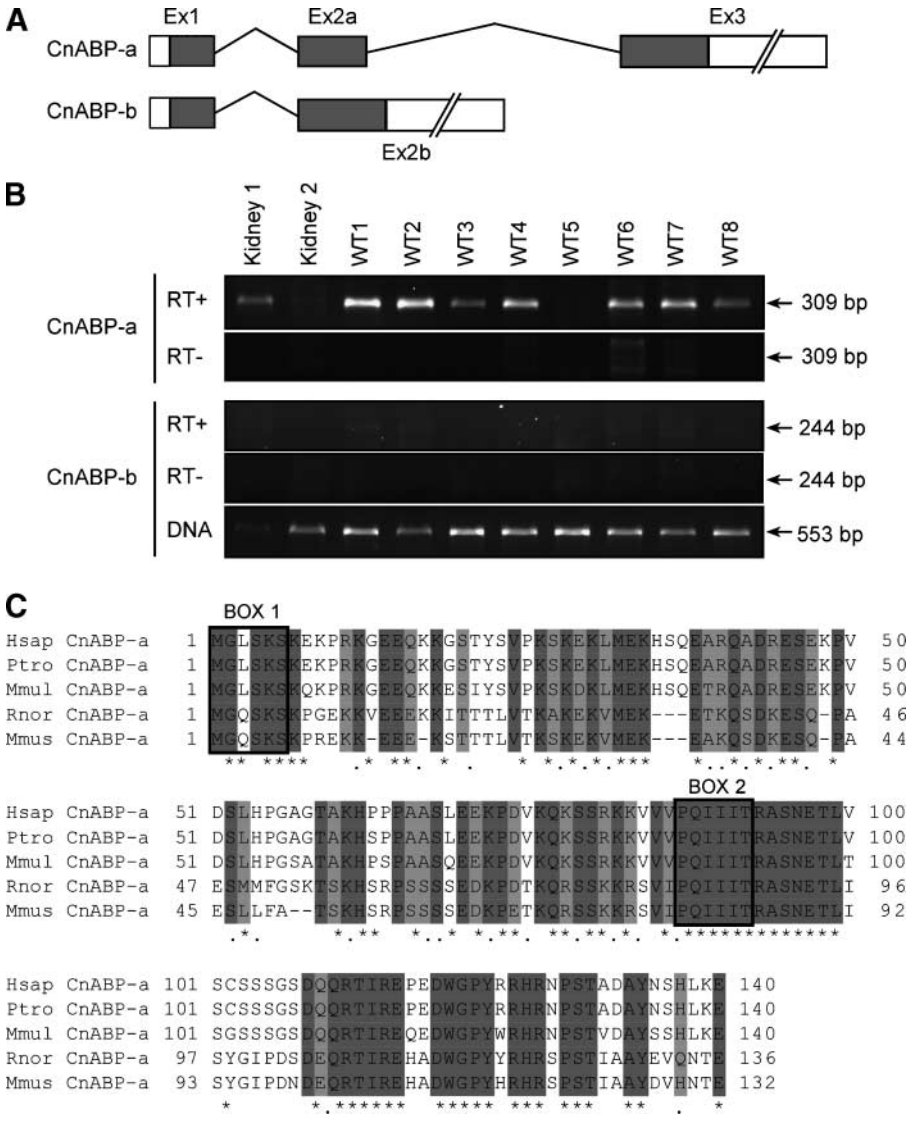

FIGURE 2. Structure and conservation of CnABP. **A.** In human, there are two main isoforms of *CnABP*. Isoform-a contains three exons and represents >80% of *CnABP* transcripts detected in EST databases, whereas isoform-b contains two exons and represents <20%. Gray areas, predicted coding sequences. **B.** Isoform-a was consistently detected in normal kidney and WTs by PCR on reverse-transcribed cDNA, whereas isoform-b was undetectable. Genomic DNA was used as positive controls showing successful amplification of isoform-b DNA sequence. **C.** At the amino acid level, CnABP is well conserved in mammals, including *Homo sapiens* (*Hsap*), *Pan troglodytes* (*Ptro*), *Macaca mulatta* (*Mmul*), *Rattus norvegicus* (*Rnor*), and *Mus musculus* (*Mmus*). Amino acids marked in dark and light gray represent identities and similarities, respectively. NH_2-terminal Box1 identifies a putative myristoylation site corresponding to consensus sequence MGXXXS. Conserved Box2 contains the calcineurin consensus docking site PxIxIT, which is only present in isoform-a.

in comparison with empty vector ($P < 0.01$), whereas high CnABP-expressing cells increased cell migration by 7-fold ($P < 0.001$; Fig. 5B). Conversely, knockdown of CnABP in ACHN cells reduced cell migration (Fig. 5A). At 35% knockdown, we observed an 8% decrease in transfilter migration, whereas 75% knockdown reduced migration by 75% ($P < 0.01$) of the control levels (Fig. 5C). These data indicate that CnABP promotes cell migration in a dose-dependent manner.

CnABP Interacts with Calcineurin Aβ and Modulates Its Activity

To gain more insight into the cellular function of CnABP, we sought to identify putative interaction partners. For this, we submitted the full-length CnABP protein to a yeast two-hybrid approach. Two independent screens, done with the LexA and Gal4 systems, led to the identification of the serine/threonine phosphatase calcineurin Aβ as one of CnABP interacting partners. To validate this interaction, we did a pull-down assay on extracts from HEK293 cells stably transfected with His/Myc-tagged CnABP using nickel beads. Western blot analysis with an anti–calcineurin Aβ antibody revealed a strong interaction between endogenous calcineurin Aβ and CnABP in cells expressing CnABP-His/Myc (Fig. 6A). The interaction between both proteins was additionally validated by immunoprecipitation with an anti-Myc antibody directed against CnABP-His/Myc (Fig. 6B). Using pull-down and immunoprecipitation, we could not confirm interaction of CnABP with other potential partners identified in the yeast two-hybrid screens.

As CnABP binding to calcineurin Aβ suggests a role for CnABP in calcineurin signaling, we next measured the effect of CnABP on calcineurin phosphatase activity based on phosphate release from a calcineurin-specific synthetic peptide (RII). The 10-fold difference in CnABP expression between cells transfected with 1.2 and 6 μg of cDNA was used to establish low (0.1) and high (1.0) relative expression levels. The comparison of CnABP and vector-transfected HEK293 cells revealed a slight reduction in calcineurin phosphatase activity in low (0.1) CnABP-expressing cells. However, high (1.0)

Published OnlineFirst June 16, 2009; DOI: 10.1158/1541-7786.MCR-08-0402

expressing cells showed a 40% reduction in phosphatase activity ($P < 0.01$; Fig. 6C). From these data, we conclude that CnABP interacts with and negatively regulates calcineurin Aβ. This interaction gives rise to the name CnABP.

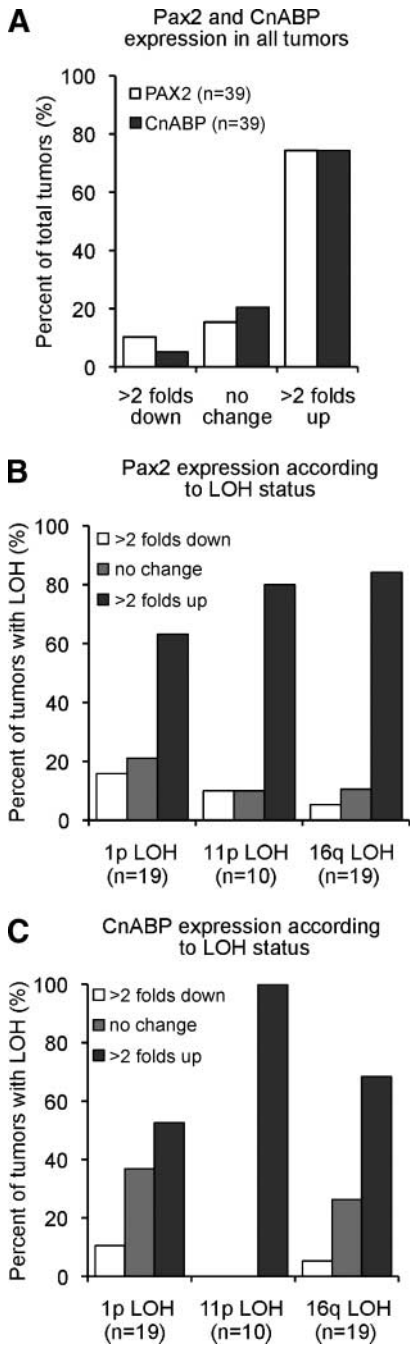

FIGURE 3. *CnABP* and *PAX2* expression in WTs. **A.** Relative quantification of *CnABP* and *PAX2* transcript levels in WTs compared with normal kidney tissues. *B2M* was used as a normalizing gene. A total of 40 tumors were tested, of which 39 tumors were informative. **B.** Expression of *PAX2* in tumors relative to normal kidney tissue is classified according to known loss of heterozygosity. **C.** *CnABP* expression in tumors was similarly grouped according to LOH status. Tumors are classified as decreased (≥2-fold) or increased (≥2-fold) in comparison with normal tissue. Change in transcript level between these cutoffs is considered unchanged.

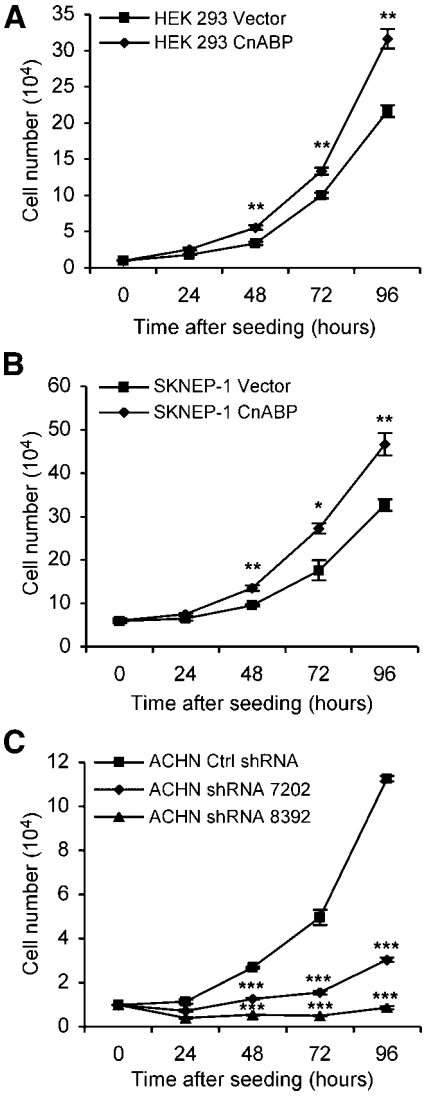

FIGURE 4. CnABP promotes cell proliferation of normal kidney and WT cell lines. **A.** Proliferation curve of human embryonic kidney 293 cells transfected with *CnABP*. At 96 h, *CnABP*-transfected cells show a 50% increase ($P < 0.01$) in cell counts compared with vector control cells. **B.** Proliferation curve of WT SKNEP-1 transfected with vector control or *CnABP*. *CnABP*-transfected SKNEP-1 cells also show a 50% increase ($P < 0.01$) in cell numbers at 96 h compared with vector control cells. **C.** *CnABP* was knocked down in ACHN cells by two shRNA (7202 and 8392). shRNA 7202 caused 70% reduction ($P < 0.001$) in cell counts after 96 h, whereas shRNA 8392 resulted in complete arrest of cell growth ($P < 0.001$). *, $P < 0.05$; **, $P < 0.01$; ***, $P < 0.001$.

CnABP Inhibits Calcineurin-Mediated Nuclear Translocation of Nuclear Factor of Activated T Cell

We next investigated whether the inhibition of calcineurin Aβ by CnABP would affect calcineurin-mediated signaling. The nuclear factor of activated T-cell (NFAT) family of transcription factors is known as one of the main signaling components downstream of calcineurin. On calcium release, calcineurin dephosphorylates NFAT, which leads to its nuclear translocation where it acts as a transcriptional regulator. To test whether CnABP affects this process, we first investigated the effect of CnABP on endogenous NFAT nuclear translocation

Published OnlineFirst June 16, 2009; DOI: 10.1158/1541-7786.MCR-08-0402

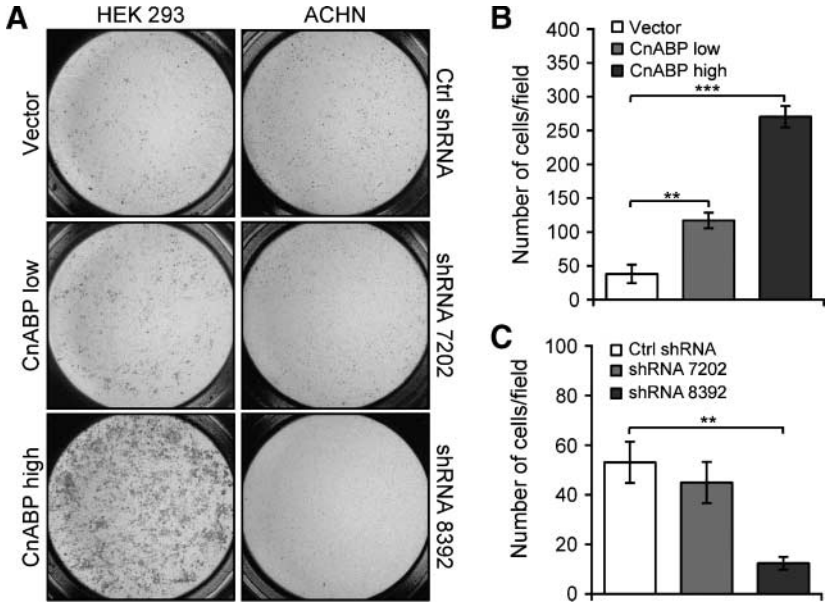

FIGURE 5. CnABP increases cell migration in a dose-dependent manner. **A.** Expression of CnABP in HEK-293 cells increases the number of cells migrated through filters. Conversely, knockdown of CnABP in ACHN cells reduces cell migration as judged by crystal violet staining. **B.** Low CnABP expression significantly increased cell migration by 3-fold ($P < 0.01$). High CnABP protein levels increased the number of cells migrated by 7-fold compared with vector control cells ($P < 0.001$). **C.** Knockdown of CnABP in ACHN cells by shRNA 7202 led to an 8% reduction (nonsignificant), whereas knockdown by shRNA 8392 resulted in 70% reduction ($P < 0.01$) of migrated cells. **, $P < 0.01$; ***, $P < 0.001$.

in HEK293 cells. In the absence of stimulus, NFATc3 is mostly cytosolic (Fig. 7A). On activating calcium release by ionomycin, NFATc3 rapidly translocates into the nucleus (Fig. 7B). In striking contrast, ionomycin treatment on CnABP-expressing cells completely failed to translocate NFATc3 to the nucleus (Fig. 7D). This inhibition is similar to the response obtained with cyclosporin A (CsA), a potent inhibitor of calcineurin (Fig. 7C).

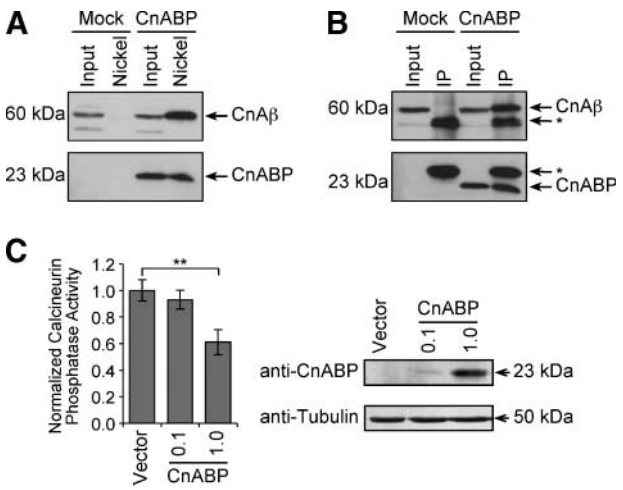

FIGURE 6. CnABP interacts with calcineurin Aβ and inhibits its phosphatase activity. Top, whole-cell extracts from HEK-293 cells expressing His/Myc-CnABP were pulled down with nickel beads (**A**) or c-Myc antibody (**B**) and analyzed by Western blot using a calcineurin Aβ antibody (*CnAβ*). Bottom, expression of His/Myc-CnABP was detected with an anti-Myc antibody. Input corresponds to 10% of protein extract used in the assay. Asterisks indicate the presence of IgGs. IP, immunoprecipitation. **C.** Cell extracts from HEK-293 expressing CnABP or an empty vector were analyzed with a malachite-based phosphatase assay to assess calcineurin-specific phosphatase activities. The levels of CnABP expression were normalized to tubulin levels using quantitative fluorescent imaging. CnABP expression correlates with reduction in calcineurin phosphatase activities. Low-level relative expression (0.1) of CnABP leads to a non-significant reduction in calcineurin phosphatase activity, whereas higher-level expression (1.0) leads to 40% reduction in activity ($P < 0.01$). **, $P < 0.01$. Full-length blots are presented in Supplementary Fig. S3.

CnABP Inhibits NFAT Transcriptional Response

We next assessed whether inhibition of calcineurin Aβ by CnABP would result in a reduction of NFAT transcriptional response. The effect of CnABP was assessed by measuring the expression of *cyclooxygenase-2* and *c-Myc*, which are two established nuclear targets of NFAT. As expected, ionomycin-dependent up-regulation of both genes could be efficiently inhibited by CnABP expression (Fig. 7E and F). To confirm that this effect is mediated through NFAT-specific transcriptional activity, we assessed the effect of CnABP on NFAT-responsive promoters driving reporter gene expression. We used two NFAT luciferase reporter constructs, the *c-Myc* (Del1) promoter (39) and the minimal *IL2* promoter containing three upstream NFAT binding sites (40). On induction by ionomycin, we observed significant increases in luciferase expression. However, treatment with CsA or expression of CnABP resulted in strong reductions in luciferase expression. Together, these data show that calcineurin A inhibition by CnABP affects downstream signaling and nuclear response through the NFAT pathway.

Discussion

The overexpression of PAX2 in renal tumors suggests that these cells adopt a developmental program taking part in the oncogenic process. However, the molecular pathways regulated by PAX2 transcriptional activity remain poorly understood. In this study, we identified a putative target gene of Pax2 in the kidney. We showed that this gene, *CnABP*, contains a PAX2-responsive enhancer and is expressed together with *Pax2* in the embryonic kidney at different stages. Importantly, both *CnABP* and *PAX2* are overexpressed in the majority of WTs tested, consistent with a role in tumorigenesis. In support of this, the expression of CnABP was shown to promote cell

Published OnlineFirst June 16, 2009; DOI: 10.1158/1541-7786.MCR-08-0402

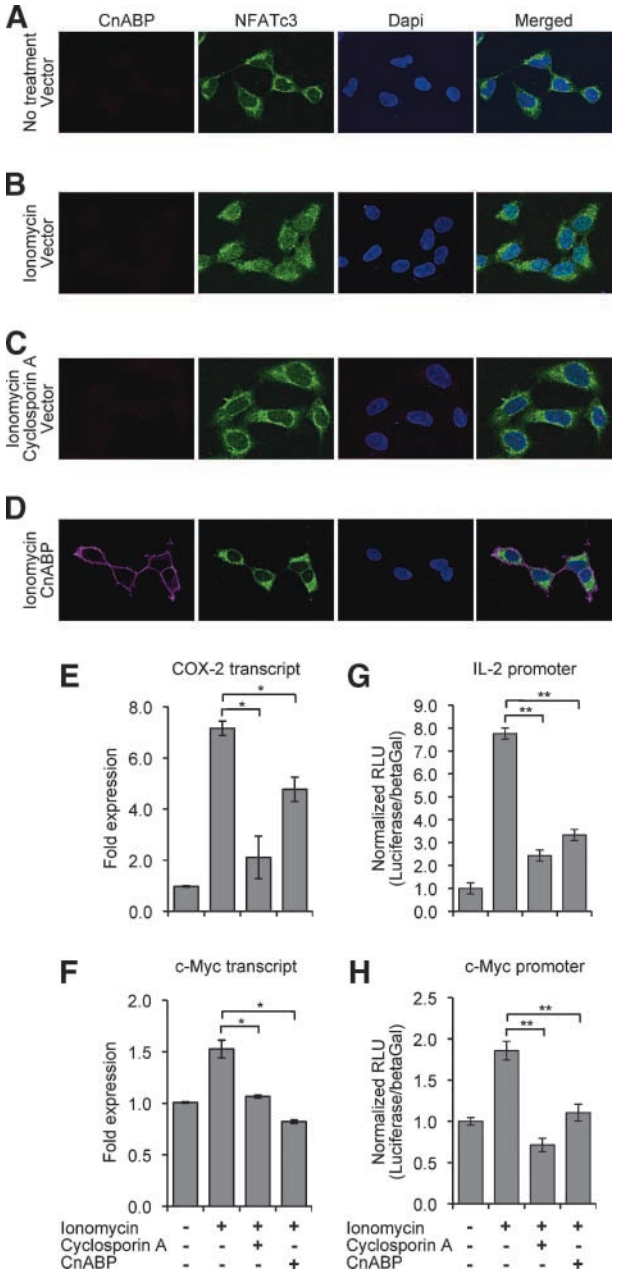

FIGURE 7. CnABP inhibits NFAT nuclear translocation and modulates NFAT transcriptional targets. **A.** Under resting condition, immunostaining for NFATc3 in HEK-293 cells shows a predominant cytoplasmic localization. **B.** Treatment of 2 μmol/L ionomycin induces calcium signaling leading to NFATc3 nuclear translocation. **C.** NFATc3 nuclear translocation is inhibited by 2 μmol/L of CsA treatment in the presence of ionomycin. **D.** CnABP expression strongly inhibits ionomycin-induced NFATc3 nuclear translocation. **E.** Ionomycin treatment increased *cyclooxygenase-2* (*COX-2*) mRNA expression levels by 8-fold compared with resting cells. The increase in *cyclooxygenase-2* mRNA level was inhibited by both CsA ($P < 0.05$) and CnABP ($P < 0.05$). **F.** Ionomycin-dependent increase in *c-Myc* transcript level was reduced to background level by both CsA ($P < 0.05$) treatment and CnABP expression ($P < 0.05$). **G.** Luciferase expression driven by the 3xNFAT-IL2 promoter showed 7.5-fold increase on ionomycin treatment. Addition of CsA or CnABP resulted in 70% ($P < 0.01$) and 60% ($P < 0.01$) reduction of luciferase expression, respectively. **H.** Luciferase expression under the control of the c-Myc (Del1) promoter exhibited 2-fold increase on ionomycin treatment. CsA or CnABP expression resulted in 60% ($P < 0.01$) and 50% ($P < 0.01$) reduction of luciferase, respectively. *, $P < 0.05$; **, $P < 0.01$.

migration and proliferation. At the molecular level, we identified CnABP as an inhibitor of calcineurin Aβ, the catalytic subunit of a phosphatase known to act as an intermediate of calcium signaling involved in proliferation and migration (41-45). Together, these results suggest a role for CnABP in the oncogenic program leading to WTs.

CnABP and WT

We find *CnABP* and *Pax2* coexpressed in the metanephric mesenchyme and other kidney compartments. Metanephric mesenchymal cells are thought to give rise to WTs when they fail to be successfully induced toward the nephron differentiation program. Strikingly, *PAX2* and *CnABP* were also coexpressed in a large proportion of the 39 WT samples we analyzed. For *PAX2*, this observation is in perfect concordance with previous studies showing overexpression in 60% to 75% of tumors (46, 47). The presence of *PAX2* and *CnABP* likely reflects the developmental origin of WTs, but the fact that they are present in such a large proportion of tumors strongly supports the idea that persistence of the developmental program participates in the oncogenic process.

Although we cannot determine exactly when CnABP exerts its action, some evidence points to a role in tumor progression rather than initiation. *CnABP* overexpression was indeed highest in WT samples with a LOH at chromosomal arms 16q and 11p, with overexpression in 70% and 100%, respectively. As LOH at 16q has been associated with later stages of tumor progression and poor prognosis (7, 8) and typically follows loss of *Wt1* at 11p15 (48), the overexpression of CnABP likely comes as a later event in tumor progression. The 2- to 18-fold overexpression of *CnABP* in 16q LOH tumors is especially remarkable in that the *CnABP* gene is located on this chromosomal segment (16q24). *CnABP* is thus highly overexpressed in those tumors in spite of the presence of a single allele instead of two. In further support of a role in tumor progression is the link between CnABP and cell migration. This is especially relevant in the context of WT recurrence observed in 15% of cases. These tumors are generally resistant to treatment regardless of histologic features and acquire the capacity to migrate and invade surrounding tissues (5, 6). This link between WT recurrence and increased cell dissemination (6) is entirely compatible with the cellular functions we identified for CnABP. Expression of CnABP in embryonic kidney and WT cell lines indeed results in a modest increase in cell proliferation but most strikingly results in a 7-fold increase in cell migration. Our results therefore suggest a potential association between CnABP overexpression and adverse prognosis that could eventually be explored in the context of therapeutic interventions.

Regulation of Calcineurin Signaling by CnABP

In an effort to better understand the molecular function of CnABP in the cell, we looked for protein partners and identified the signaling molecule calcineurin Aβ. We showed that CnABP interacts with calcineurin Aβ and interferes with its phosphatase activity as well as with its downstream NFAT-dependent nuclear response. At the cellular level, calcineurin-NFAT signaling has been associated with different outcomes such as increased proliferation and migration (42, 44, 45). This pathway was shown to play an important role

Published OnlineFirst June 16, 2009; DOI: 10.1158/1541-7786.MCR-08-0402

in kidney development (49) and homeostasis (50). Interestingly, a number of calcineurin pathway components, including calcineurin A, were recently identified as specifically up-regulated in relapsing WTs (9). The calcineurin pathway itself may thus be involved in WT progression. Our results suggest that CnABP overexpression in WTs might impinge on this pathway.

In our experiments, the interaction between CnABP and calcineurin A leads to an inhibition of calcineurin phosphatase activity. This is somewhat surprising because both CnABP and calcineurin pathway activation are linked to promigratory and proproliferative activities. One possibility is that the nuclear response to NFAT signaling may not be as straightforward as previously thought. In this respect, it is interesting to note that NFATc3, which we found regulated by CnABP, may act as a tumor suppressor in certain systems and thus have antiproliferative activity (51, 52). Similarly, calcineurin regulation of NFATc2 inhibits cyclin-dependent kinase 4 expression, a cyclin-dependent kinase promoting reentry into the cell cycle (53). Hence, calcineurin signaling seems to have both proproliferative and antiproliferative activities depending on the cellular context. It is also possible that CnABP is involved in calcineurin-independent promigratory/proproliferative pathways yet to be identified. Alternatively, it is possible that CnABP is a substrate for calcineurin with its own NFAT-independent cellular activity, as is the case for the K^+ channel TRESK (54). In this respect, it is remarkable that the best-conserved domain of CnABP contains a perfect PxIxIT consensus sequence (where x represents any amino acid), which is a calcineurin docking site found in NFATs and other calcineurin substrates (54, 55), as well as in calcineurin inhibitor proteins such as Cain/Cabin1 and A238L (56-58). This sequence was shown to be sufficient for binding to calcineurin (59). In fact, based on a mapped consensus binding strength, the PQIIIT sequence of CnABP is predicted as a strong binding site among calcineurin binding partners or substrates (59). Mutagenesis experiments will be important to determine the exact role of this site in CnABP function. The details of the intriguing relationship between CnABP and calcineurin signaling remain to be clarified and will be the focus of further studies.

Materials and Methods

Pax2 Target Gene Identification

The identification of Pax2 target genes in the mesonephros was described elsewhere (36). Briefly, mesonephric cells from C3H/He embryos were sorted by flow cytometry using a bacterial artificial chromosome transgene expressing GFP under the control of the *Pax2* locus. Total RNA from sorted cells was submitted to linear amplification and hybridized to cDNA microarrays containing 25,000 ESTs. Sample comparisons were wild-type to *Pax2* mutant, GFP-positive mesonephros to surrounding GFP-negative tissue, as well as samples from different stages of mesonephros development.

PAX2-Binding Sites

A region spanning 50 kb upstream to 50 kb downstream of the human *CnABP* gene was used to map potential PBSs. Sites were chosen based on sequence conservation between human and mouse or rat. Three PBSs (−7267, +2012, and +5698) were named PBS1, PBS2, and PBS3, respectively. A region of 200 bp surrounding each site was cloned into pGL3 vector upstream of a TATA box and firefly luciferase cDNA. Mutations to three critical base pairs were engineered into PBS2 by site-directed mutagenesis (Fig. 1A).

Luciferase Assay

Cells in 12-well plates were transiently transfected with 0.25 μg of reporter plasmids and 0.25 μg of expression constructs with 0.01 μg of pCMV-βGAL as transfection control using Fugene (Roche). To test for PAX2 activation of putative PBSs, pGL3-PBS1, pGL3-PBS2, pGL3-PBS3, and pGL3-PBS2-Mut were transfected with pCDNA3.1 or pCDNA3.1-PAX2 (a gift from Dr. Paul Goodyer, McGill University, Montreal, Canada). To evaluate the effect of CnABP on NFAT-responsive promoters, pGL3-NFAT-Luc (40) and pBV-cMyc (Del1; ref. 39) were transfected with pCDNA4 or pCDNA4-CnABP. Treatment of 2 μmol/L ionomycin and/or 2 μmol/L CsA was administered 24 h after transfection. Forty-eight hours after transfection, cell lysates were collected. Luciferase activity was determined by luciferase assay (Promega) using a luminometer (Luminoskan, Thermo). Relative light units were normalized against β-galactosidase staining and vector control.

In situ *Hybridization*

In situ hybridization was done as described previously (60). *CnABP* cRNA probe was generated from IMAGE clone ID 6771161 (Invitrogen), containing the full coding sequence. *Pax2* cRNA probe was described previously (61, 62).

WT Samples

Thirty-nine WT and 2 normal kidney samples were obtained from the Children Oncology Group (Arcadia, CA). All but one tumor were removed before chemotherapeutic treatment and were previously characterized by the Children Oncology Group for LOH at positions 16q, 1p, and 11p. Tumors and normal tissues were obtained in respect of institutional and national bioethical guidelines.

Reverse Transcription-PCR and Quantitative Real-time PCR

RNA from frozen tumor samples or from cells in culture was extracted with Trizol (Invitrogen). cDNA was synthesized by reverse transcription of 1 μg RNA using SuperScript II (Invitrogen). Expression analysis of *CnABP* isoform-a and isoform-b was done by PCR on reverse-transcribed cDNA with isoform-specific primers. Genomic DNA was used as positive control for isoform-b. All quantitative PCRs were done in duplicates on a Light Cycler (Roche) using SYBR Green (Sigma) as detection method. Primers used to amplify human *CnABP* are as follows: isoform-a, 5′-GAGAAGTTGATGGAGAAGCATTCC-3′ (+83 to +105; forward) and 5′-TGCTGTACTGGGGTTCCTGTGC-3′ (+369 to +390; reverse); isoform-b, 5′-AAAGCAAAGA-GAAACCCAGGAAAG-3′ (+53 to +76; forward) and 5′-CCTCCAAGCCACTGACCTCG-3′ (+277 to +296; reverse). Primers used to amplify human *cyclooxygenase-2* are 5′-AACACCCTCTATCACTGGCATCC-3′ (forward) and 5′-CCTGCTCTGGTCAATGGAAGC-3′ (reverse). Primers used to amplify *c-Myc* (63), *PAX2*, and *β2-microglobulin* (*B2M*; ref. 27) were described previously. Relative expression of

Published OnlineFirst June 16, 2009; DOI: 10.1158/1541-7786.MCR-08-0402

mRNA transcripts was calculated with respect to *B2M* transcript levels.

Overexpression and Knockdown of CnABP

Cell lines used (HEK-293, SKNEP-1, and ACHN) were obtained from the American Type Culture Collection. The HEK-293 cell line was maintained in DMEM (Wisent) supplemented with 10% fetal bovine serum (Wisent), SKNEP-1 WT cell line was maintained in McCoy's 5A (Wisent) supplemented with 15% fetal bovine serum, and ACHN renal cell carcinoma cell line was maintained in Eagle's MEM (Wisent) supplemented with 0.1 mmol/L nonessential amino acids, 1 mmol/L sodium pyruvate, and 10% fetal bovine serum. Wild-type coding sequence of *CnABP* was PCR amplified from human *CnABP* cDNA clone obtained from the Image Clone Collection (ID 2688932; Invitrogen) and cloned into pCDNA4/Myc-His A (Invitrogen). Myc-His–tagged CnABP was generated by site-directed mutagenesis of *CnABP* stop codon in pCDNA4/Myc-His A. Cells were either transiently transfected or selected as pools with zeocine (Invitrogen) for 2 wk before doing functional assays. Knockdown of *CnABP* was achieved by lentiviral-mediated expression of shRNA targeting *CnABP* transcript. shRNA hairpins expressed in pLKO.1 were obtained from Open Biosystems (IMAGE IDs: TRCN0000137202 and TRCN0000138392). Viral particles were collected 48 h after transfection for up to 7 d. Cells were infected daily with filtered virus (0.45 μm filters, PALL) and 4 μg/mL polybrene. Infected cells were selected with 2 ng/mL puromycin (Calbiochem) for 2 wk before doing functional assays. Experiments done with lentivirus were carried out according to institutional guidelines.

Western Blot Analysis

Western blot was done according to standard procedure. Rabbit polyclonal anti-CnABP antibodies were generated by injection of a 21–amino acid synthetic peptide corresponding to the COOH terminus of CnABP. Antibody specificity for endogenous and transfected CnABP was tested by peptide competition at 10× or 100× the concentration of the antibodies used. Concentrations used for Western blot analysis were 1:1,000 for anti-CnABP and 1:1,000 for anti-tubulin (Abcam). Secondary antibodies conjugated to horseradish peroxidase (1:10,000; Amersham) and enhanced chemiluminescence Plus reagent (Amersham) were used for detection. Stripping of blots was done using Re-Blot Plus Strong Solution (Chemicon).

Cell Proliferation Assay

Experimental and control cells were plated at densities of 10,000 per well (HEK-293 and ACHN) or 50,000 per well (SKNEP-1) in 12-well plates. Cells were counted using Coulter counter over 4 d; each time point was measured in triplicates. Statistical values were obtained with Student's *t* test.

Cell Migration Assay

Transwell filter assay was done as previously described (64). Cells (HEK-293 and ACHN) were seeded on 8-μm polycarbon filters with serum-free medium. Complete medium is added below the filters. Cells were allowed to migrate for 24 to 48 h at 37°C, 5% CO_2. Filters were fixed in 10% formalin and stained with crystal violet solution (0.1% crystal violet, 20% methanol). Nonmigratory cells were manually removed with cotton tips. Each experiment was done in triplicates and four fields of 1 mm^2 were used to quantify the number of migrated cells.

Yeast Two-Hybrid Assays

Yeast two-hybrid assays were done in collaboration with Hybrigenics. For this, the full-length *CnABP* bait was expressed in frame with LexA or Gal4DBD and each construct was screened against an embryonic cDNA library. Calcineurin Aβ was identified in both LexA- and Gal4AD-based screens.

Pull-Down and Immunoprecipitation

Cells were lysed in binding buffer containing 20 mmol/L Tris (pH 8), 25 mmol/L NaCl, 1% Triton X-100, 10% glycerol, and protease inhibitors (Roche). Histidine-tagged CnABP was pulled down with Ni Sepharose 6 Fast Flow beads (Amersham) according to the manufacturer's instructions. Immunoprecipitation was done overnight with c-Myc antibody (clone 9E10; Santa Cruz Biotechnology) and incubated for the last 4 h with protein A/G Plus-agarose beads (Santa Cruz Biotechnology). The beads were washed thrice with binding buffer and proteins were resolved by SDS-PAGE. Western blots were done with calcineurin Aβ (1:1,000; Upstate) and c-Myc (1:1,000; Upstate) antibodies.

Calcineurin Phosphatase Assay

The calcineurin activity assay was done using the Calcineurin Cellular Assay Kit Plus (Biomol International) according to the manufacturer's instructions. The assay was made in HEK-293 cells transfected with different amounts (1.2 and 6 μg) of CnABP or pCDNA4/Myc-His vector DNA using Fugene 6 (Roche) according to the manufacturer's instructions. Western blot using Alexa-conjugated secondary antibodies and the Typhoon detection system (Amersham) were used to quantify the level of CnABP expression. *P* values were obtained by Student's *t* test.

Immunocytochemistry

For immunofluorescence staining, cover slides were pretreated with 12 N HCl for 5 min, washed with water, and dried in an oven at 60°C overnight. Cells (250,000) were plated in six-well plates and allowed to rest for 24 h. Cells were then transfected with either CnABP or pCDNA4/Myc-His A control vector. Twenty-four hours after transfection, the cells were treated with 2 μmol/L ionomycin and/or 2 μmol/L CsA for 15 min. Cells were briefly rinsed with PBS and fixed in 4% paraformaldehyde for 15 min. Samples were blocked with 10% normal goat serum and 0.2% Triton X-100 in PBS for 1 h at room temperature. Slides were incubated with anti-NFATc3 (1:50; Santa Cruz Biotechnology) and/or anti-Myc (1:100; Upstate) in 1% normal goat serum and 0.2% Triton X-100 in PBS overnight at 4°C. Subsequently, samples were incubated with Alexa-labeled secondary antibodies (Invitrogen) and 1 μg/mL of 4′,6-diamidino-2-phenylindole for 1 h at room temperature. Cells were washed thrice with PBS for 10 min between each step. Samples were mounted on cover slides using Prolong Antifade mounting medium (Invitrogen) and cured overnight at room temperature. Images were obtained on a LSM 5 Pascal confocal microscope (Zeiss).

Published OnlineFirst June 16, 2009; DOI: 10.1158/1541-7786.MCR-08-0402

Disclosure of Potential Conflicts of Interest

The authors declare no conflicts of interest.

Acknowledgments

We thank the Children Oncology Group and the Cooperative Human Tissue Network for providing WT samples, Hybrigenics for the yeast two-hybrid assay, and Jerry Pelletier and Arnim Pause and the members of the Bouchard lab for critical reading of the manuscript.

References

1. Rivera MN, Haber DA. Wilms' tumour: connecting tumorigenesis and organ development in the kidney. Nat Rev Cancer 2005;5:699–712.

2. Li CM, Guo M, Borczuk A, et al. Gene expression in Wilms' tumor mimics the earliest committed stage in the metanephric mesenchymal-epithelial transition. Am J Pathol 2002;160:2181–90.

3. Jones KP, Grundy PE, Coppes MJ. Recent advances in the genetics of childhood renal cancers: a report of the 3rd International Conference on the molecular and clinical genetics of childhood renal tumors, together with the Mitchell Ross symposium on anaplastic and other high risk embryonal tumors of childhood, 8-10th April 1999, Wistar Institute, Philadelphia, PA. Med Pediatr Oncol 2000; 35:126–30.

4. Grundy P, Breslow N, Green DM, Sharples K, Evans A, D'Angio GJ. Prognostic factors for children with recurrent Wilms' tumor: results from the Second and Third National Wilms' Tumor Study. J Clin Oncol 1989;7:638–47.

5. Bonadio JF, Storer B, Norkool P, Farewell VT, Beckwith JB, D'Angio GJ. Anaplastic Wilms' tumor: clinical and pathologic studies. J Clin Oncol 1985;3: 513–20.

6. Beckwith JB, Palmer NF. Histopathology and prognosis of Wilms tumors: results from the First National Wilms' Tumor Study. Cancer 1978;41:1937–48.

7. Grundy PE, Telzerow PE, Breslow N, Moksness J, Huff V, Paterson MC. Loss of heterozygosity for chromosomes 16q and 1p in Wilms' tumors predicts an adverse outcome. Cancer Res 1994;54:2331–3.

8. Grundy RG, Pritchard J, Scambler P, Cowell JK. Loss of heterozygosity on chromosome 16 in sporadic Wilms' tumour. Br J Cancer 1998;78:1181–7.

9. Li W, Kessler P, Yeger H, et al. A gene expression signature for relapse of primary Wilms tumors. Cancer Res 2005;65:2592–601.

10. Call KM, Glaser T, Ito CY, et al. Isolation and characterization of a zinc finger polypeptide gene at the human chromosome 11 Wilms' tumor locus. Cell 1990;60:509–20.

11. Gessler M, Poustka A, Cavenee W, Neve RL, Orkin SH, Bruns GA. Homozygous deletion in Wilms tumours of a zinc-finger gene identified by chromosome jumping. Nature 1990;343:774–8.

12. Haber DA, Buckler AJ, Glaser T, et al. An internal deletion within an 11p13 zinc finger gene contributes to the development of Wilms' tumor. Cell 1990;61: 1257–69.

13. Pelletier J, Bruening W, Kashtan CE, et al. Germline mutations in the Wilms' tumor suppressor gene are associated with abnormal urogenital development in Denys-Drash syndrome. Cell 1991;67:437–47.

14. Varanasi R, Bardeesy N, Ghahremani M, et al. Fine structure analysis of the WT1 gene in sporadic Wilms tumors. Proc Natl Acad Sci U S A 1994;91:3554–8.

15. Kikuchi H, Akasaka Y, Nagai T, et al. Genomic changes in the WT-gene (WT1) in Wilms' tumors and their correlation with histology. Am J Pathol 1992;140:781–6.

16. Kreidberg JA, Sariola H, Loring JM, et al. WT-1 is required for early kidney development. Cell 1993;74:679–91.

17. Donovan MJ, Natoli TA, Sainio K, et al. Initial differentiation of the metanephric mesenchyme is independent of WT1 and the ureteric bud. Dev Genet 1999;24:252–62.

18. Davies JA, Ladomery M, Hohenstein P, et al. Development of an siRNA-based method for repressing specific genes in renal organ culture and its use to show that the Wt1 tumour suppressor is required for nephron differentiation. Hum Mol Genet 2004;13:235–46.

19. Dressler GR, Douglass EC. Pax-2 is a DNA-binding protein expressed in embryonic kidney and Wilms tumor. Proc Natl Acad Sci U S A 1992;89:1179–83.

20. Poleev A, Fickenscher H, Mundlos S, et al. PAX8, a human paired box gene: isolation and expression in developing thyroid, kidney and Wilms' tumors. Development 1992;116:611–23.

21. Eccles MR, Yun K, Reeve AE, Fidler AE. Comparative *in situ* hybridization analysis of PAX2, PAX8, and WT1 gene transcription in human fetal kidney and Wilms' tumors. Am J Pathol 1995;146:40–5.

22. Ryan G, Steele-Perkins V, Morris JF, Rauscher F, Jr., Dressler GR. Repression of Pax-2 by WT1 during normal kidney development. Development 1995; 121:867–75.

23. Dehbi M, Ghahremani M, Lechner M, Dressler G, Pelletier J. The paired-box transcription factor, PAX2, positively modulates expression of the Wilms' tumor suppressor gene (WT1). Oncogene 1996;13:447–53.

24. Brophy PD, Ostrom L, Lang KM, Dressler GR. Regulation of ureteric bud outgrowth by Pax2-dependent activation of the glial derived neurotrophic factor gene. Development 2001;128:4747–56.

25. Narlis M, Grote D, Gaitan Y, Boualia SK, Bouchard M. Pax2 and pax8 regulate branching morphogenesis and nephron differentiation in the developing kidney. J Am Soc Nephrol 2007;18:1121–9.

26. Gnarra JR, Dressler GR. Expression of Pax-2 in human renal cell carcinoma and growth inhibition by antisense oligonucleotides. Cancer Res 1995;55:4092–8.

27. Muratovska A, Zhou C, He S, Goodyer P, Eccles MR. Paired-Box genes are frequently expressed in cancer and often required for cancer cell survival. Oncogene 2003;22:7989–97.

28. Hueber PA, Waters P, Clark P, Eccles M, Goodyer P. PAX2 inactivation enhances cisplatin-induced apoptosis in renal carcinoma cells. Kidney Int 2006;69: 1139–45.

29. Fonsato V, Buttiglieri S, Deregibus MC, Puntorieri V, Bussolati B, Camussi G. Expression of Pax2 in human renal tumor-derived endothelial cells sustains apoptosis resistance and angiogenesis. Am J Pathol 2006;168:706–13.

30. Ostrom L, Tang MJ, Gruss P, Dressler GR. Reduced Pax2 gene dosage increases apoptosis and slows the progression of renal cystic disease. Dev Biol 2000;219:250–8.

31. Porteous S, Torban E, Cho NP, et al. Primary renal hypoplasia in humans and mice with PAX2 mutations: evidence of increased apoptosis in fetal kidneys of Pax2(1Neu) +/− mutant mice. Hum Mol Genet 2000;9:1–11.

32. Torban E, Eccles MR, Favor J, Goodyer PR. PAX2 suppresses apoptosis in renal collecting duct cells. Am J Pathol 2000;157:833–42.

33. Bouchard M, Pfeffer P, Busslinger M. Functional equivalence of the transcription factors Pax2 and Pax5 in mouse development. Development 2000; 127:3703–13.

34. Buttiglieri S, Deregibus MC, Bravo S, et al. Role of Pax2 in apoptosis resistance and proinvasive phenotype of Kaposi's sarcoma cells. J Biol Chem 2004; 279:4136–43.

35. Igarashi T, Ueda T, Suzuki H, et al. Aberrant expression of Pax-2 mRNA in renal cell carcinoma tissue and parenchyma of the affected kidney. Int J Urol 2001;8:60–4.

36. Grote D, Souabni A, Busslinger M, Bouchard M. Pax2/8-regulated Gata3 expression is necessary for morphogenesis and guidance of the nephric duct in the developing kidney. Development 2006;133:53–61.

37. Gaitan Y, Bouchard M. Expression of the δ-protocadherin gene Pcdh19 in the developing mouse embryo. Gene Expr Patterns 2006;6:893–9.

38. Dome JS, Coppes MJ. Recent advances in Wilms tumor genetics. Curr Opin Pediatr 2002;14:5–11.

39. He TC, Sparks AB, Rago C, et al. Identification of c-MYC as a target of the APC pathway. Science 1998;281:1509–12.

40. Clipstone NA, Crabtree GR. Identification of calcineurin as a key signalling enzyme in T-lymphocyte activation. Nature 1992;357:695–7.

41. Zaninetti R, Tacchi S, Erriquez J, et al. Calcineurin primes immature GnRH-secreting neuroendocrine cells for migration. Mol Endocrinol 2007.

42. Buchholz M, Ellenrieder V. An emerging role for Ca^{2+}/calcineurin/NFAT signaling in cancerogenesis. Cell Cycle 2007;6:16–9.

43. Buchholz M, Schatz A, Wagner M, et al. Overexpression of c-myc in pancreatic cancer caused by ectopic activation of NFATc1 and the Ca^{2+}/calcineurin signaling pathway. EMBO J 2006;25:3714–24.

44. Eckstein LA, Van Quill KR, Bui SK, Uusitalo MS, O'Brien JM. Cyclosporin a inhibits calcineurin/nuclear factor of activated T-cells signaling and induces apoptosis in retinoblastoma cells. Invest Ophthalmol Vis Sci 2005;46:782–90.

45. Corral RS, Iniguez MA, Duque J, Lopez-Perez R, Fresno M. Bombesin induces cyclooxygenase-2 expression through the activation of the nuclear factor of activated T cells and enhances cell migration in Caco-2 colon carcinoma cells. Oncogene 2007;26:958–69.

46. Tagge EP, Hanson P, Re GG, Othersen HB, Jr., Smith CD, Garvin AJ. Paired box gene expression in Wilms' tumor. J Pediatr Surg 1994;29:134–41.

47. Eccles MR, Wallis LJ, Fidler AE, Spurr NK, Goodfellow PJ, Reeve AE. Expression of the PAX2 gene in human fetal kidney and Wilms' tumor. Cell Growth Differ 1992;3:279–89.

Published OnlineFirst June 16, 2009; DOI: 10.1158/1541-7786.MCR-08-0402

48. Charles AK, Brown KW, Berry PJ. Microdissecting the genetic events in nephrogenic rests and Wilms' tumor development. Am J Pathol 1998;153:991–1000.

49. Tendron A, Decramer S, Justrabo E, Gouyon JB, Semama DS, Gilbert T. Cyclosporin A administration during pregnancy induces a permanent nephron deficit in young rabbits. J Am Soc Nephrol 2003;14:3188–96.

50. Myers BD, Ross J, Newton L, Luetscher J, Perlroth M. Cyclosporine-associated chronic nephropathy. N Engl J Med 1984;311:699–705.

51. Glud SZ, Sorensen AB, Andrulis M, et al. A tumor-suppressor function for NFATc3 in T-cell lymphomagenesis by murine leukemia virus. Blood 2005;106:3546–52.

52. Lee H, Chouinard L, Bonin M, Michel RN. NFATc3 deficiency may contribute to the development of mammary gland adenocarcinoma in aging female mice. Mol Carcinog 2005;44:219–22.

53. Baksh S, Widlund HR, Frazer-Abel AA, et al. NFATc2-mediated repression of cyclin-dependent kinase 4 expression. Mol Cell 2002;10:1071–81.

54. Czirjak G, Enyedi P. Targeting of calcineurin to an NFAT-like docking site is required for the calcium-dependent activation of the background K^+ channel, TRESK. J Biol Chem 2006;281:14677–82.

55. Aramburu J, Garcia-Cozar F, Raghavan A, Okamura H, Rao A, Hogan PG. Selective inhibition of NFAT activation by a peptide spanning the calcineurin targeting site of NFAT. Mol Cell 1998;1:627–37.

56. Lai MM, Burnett PE, Wolosker H, Blackshaw S, Snyder SH. Cain, a novel physiologic protein inhibitor of calcineurin. J Biol Chem 1998;273:18325–31.

57. Miskin JE, Abrams CC, Dixon LK. African swine fever virus protein A238L interacts with the cellular phosphatase calcineurin via a binding domain similar to that of NFAT. J Virol 2000;74:9412–20.

58. Sun L, Youn HD, Loh C, Stolow M, He W, Liu JO. Cabin 1, a negative regulator for calcineurin signaling in T lymphocytes. Immunity 1998;8:703–11.

59. Li H, Zhang L, Rao A, Harrison SC, Hogan PG. Structure of calcineurin in complex with PVIVIT peptide: portrait of a low-affinity signalling interaction. J Mol Biol 2007;369:1296–306.

60. Henrique D, Adam J, Myat A, Chitnis A, Lewis J, Ish-Horowicz D. Expression of a Delta homologue in prospective neurons in the chick. Nature 1995;375:787–90.

61. Bouchard M, Souabni A, Mandler M, Neubuser A, Busslinger M. Nephric lineage specification by Pax2 and Pax8. Genes Dev 2002;16:2958–70.

62. Buckler AJ, Pelletier J, Haber DA, Glaser T, Housman DE. Isolation, characterization, and expression of the murine Wilms' tumor gene (WT1) during kidney development. Mol Cell Biol 1991;11:1707–12.

63. Kunz F, Shalaby T, Lang D, et al. Quantitative mRNA expression analysis of neurotrophin-receptor TrkC and oncogene c-MYC from formalin-fixed, paraffin-embedded primitive neuroectodermal tumor samples. Neuropathology 2006;26:393–9.

64. Kurban G, Hudon V, Duplan E, Ohh M, Pause A. Characterization of a von Hippel Lindau pathway involved in extracellular matrix remodeling, cell invasion, and angiogenesis. Cancer Res 2006;66:1313–9.

AACR American Association for Cancer Research

Molecular Cancer Research

Calcineurin A–Binding Protein, a Novel Modulator of the Calcineurin-Nuclear Factor of Activated T-Cell Signaling Pathway, Is Overexpressed in Wilms' Tumors and Promotes Cell Migration

Alana H.T. Nguyen, Mélanie Béland, Yaned Gaitan, et al.

Mol Cancer Res 2009;7:821-831. Published OnlineFirst June 16, 2009.